



Parameter Optimization in the Thermo-mechanical V-Bending Process to Minimize Springback of Inconel 625 Alloy

Anand Badrish¹ · Ayush Morchhale¹ · Nitin Kotkunde¹ · Swadesh Kumar Singh²

Received: 5 October 2019 / Accepted: 1 February 2020 / Published online: 15 February 2020
© King Fahd University of Petroleum & Minerals 2020

Abstract

The present research deals with experimental and finite element analysis for minimization of springback in the V-bending process for Inconel 625 alloy. Different material properties were determined at three distinct temperatures (303 K, 473 K and 673 K) and deformation speeds (1 mm/min, 5 mm/min and 10 mm/min). Temperature was found to have significant effect on the flow stress of the material. Taguchi analysis was applied to find springback of Inconel 625 by considering four process parameters (temperature, punch speed, holding time and orientation of the sheet) and at the three predetermined levels of settings. Based upon signal-to-noise ratio analysis, temperature (46.93%) was found to be the most influential parameter affecting the springback followed by holding time (26.29%), sheet orientation (24.07%) and punch speed (2.69%). The optimized setting for the minimum springback of Inconel 625 alloy obtained after the conformation test was 673 K temperature, 1 mm/min punch speed, 90 s holding time and 90° to the rolling direction of a sheet. The springback was significantly reduced by 69.63% with the optimized setting of process parameters. The springback factor was also evaluated, and it was found to be directly proportional to the temperature and holding time and inversely proportional to the punch speed, but no particular trend was followed for the sheet orientation as a process parameter. The Arrhenius constitutive model with both Barlat and Hill yield criteria was implemented by adopting user-defined material (UMAT) subroutine for finite element analysis. Numerically computed springback from Barlat criterion was found to be in good relation with the experimental results.

Keywords Inconel 625 alloy · V-bending · Springback · Thermo-mechanical process parameters · Taguchi analysis · Finite element analysis

1 Introduction

Inconel is a nickel-based alloy, widely used in aerospace, nuclear, marine and petrochemical industries. It possesses an excellent combination of properties at high temperatures such as high strength, ductility and corrosion resistance [1]. It also shows good weldability and creep-resistant properties which make its use possible in pumps and other equipment subjected to high pressures [2]. Welding and traditional machining operations are costly, and as a result, mass production of components using sheet metal forming is an effective alternative solution. Traditional metals such as

aluminum and steel show good forming ability when compared to Inconel alloys at room temperature (RT) as the latter possesses limited workability and drawability in cold working conditions [3, 4]. Hot or warm forming is an alternative solution to overcome such difficulties [5].

In the case of sheet metal forming, elastic recovery is a major problem when the unloading of the tool takes place. The springback effect creates major issues at the time of assembly and is mainly associated with tool design, forming conditions and material properties of the processed metal. Design of experiments (DOE) using the Taguchi method can be used to determine the combined effect of different process parameters over desired output. In order to minimize springback, an optimal set of process parameters can be determined with the help of signal-to-noise (S/N) ratio, and individual effects of process parameters over springback can be determined with the help of analysis of variance (ANOVA). Zhang et al. [6] demonstrated the Young's modulus influence over the springback effect for an aluminum alloy in

✉ Nitin Kotkunde
nitink@hyderabad.bits-pilani.ac.in

¹ Mechanical Engineering Department, BITS, Hyderabad, India

² Mechanical Engineering Department, GRIET, Hyderabad, India



the U-bending. Ramadass et al. [7] considered sheet thickness, die opening and punch radius as the process parameters for titanium grade 2 material and, based on Taguchi (L_9) orthogonal array, found sheet thickness to be the most influential parameter on springback. Bakhshi et al. [8] considered CK67 steel sheets for V-bending and found sheet thickness to be the most affecting parameter for springback. Zong et al. [9] analyzed a titanium alloy (Ti–6Al–4 V) in the V-bending process by studying the effect of holding time and punch radius over spring-go (forward) and springback effects within different temperature ranges (RT to 850 °C). Thipprakamas et al. [10] employed ANOVA and Taguchi analysis in the V-bending process of aluminum (A1100) for studying the effect of punch radius, material thickness and bending angle on spring-go and springback, identifying punch radius to be the most influential parameter. Verma et al. [11] studied the effect of anisotropy and found that springback increased with anisotropy of sheet metal. The authors further suggested to use steel sheet with thickness of approximately 1.5 mm for reduction in springback. Various thermo-mechanical process parameters have thus been observed to affect the springback behavior during the bending process [12]. The summary of these parameters in the form of a cause and effect diagram (Ishikawa diagram) is shown in Fig. 1.

In order to minimize the springback effect, a rigorous trial and error experimental process can be replaced by a finite element analysis (FEA) to save time and reduce the processing cost of sheet metals. With the development of simulation algorithms and material models with high accuracy, the FEA prediction ability improved manifold.

Panthi et al. [13] developed and employed an FEA algorithm, namely total-elastic–incremental-plastic (TE–IP) for V-bending of aluminum sheets and found friction to be the least influential parameter over springback. Thipprakamas et al. [14] studied the phenomenon of springback and spring-go in the V-bending process for aluminum (A1100) using FEA. They observed that the spring-go phenomenon is inversely proportional to punch radius, while the springback effect is directly proportional to punch radius. Narasimhan et al. [15] employed coupled explicit–implicit FEA, which in turn helped in designing a proper die for V-bending. Forcellese et al. [16] analyzed springback effect in V-bending by using FEA, in which they considered loading step as explicit and unloading step as implicit analysis and observed punch nose radius to be the most influential parameter.

From an extensive literature survey, it has been observed that much work had been done for springback analysis of traditional metals such as titanium, steel and aluminum. However, no work is available for springback analysis of high-strength alloys such as Inconel. Hence, in the present work, the springback analysis of Inconel 625 was carried out with the help of Taguchi (L_{27}) orthogonal array. Four different process parameters were considered—temperature, holding time, rolling direction and punch speed—with three levels for Taguchi analysis. ANOVA was carried out in order to determine the most influential parameter for springback. FEA is performed using user-defined material (UMAT) subroutine in ABAQUS 6.13 software for validation of experimental results.

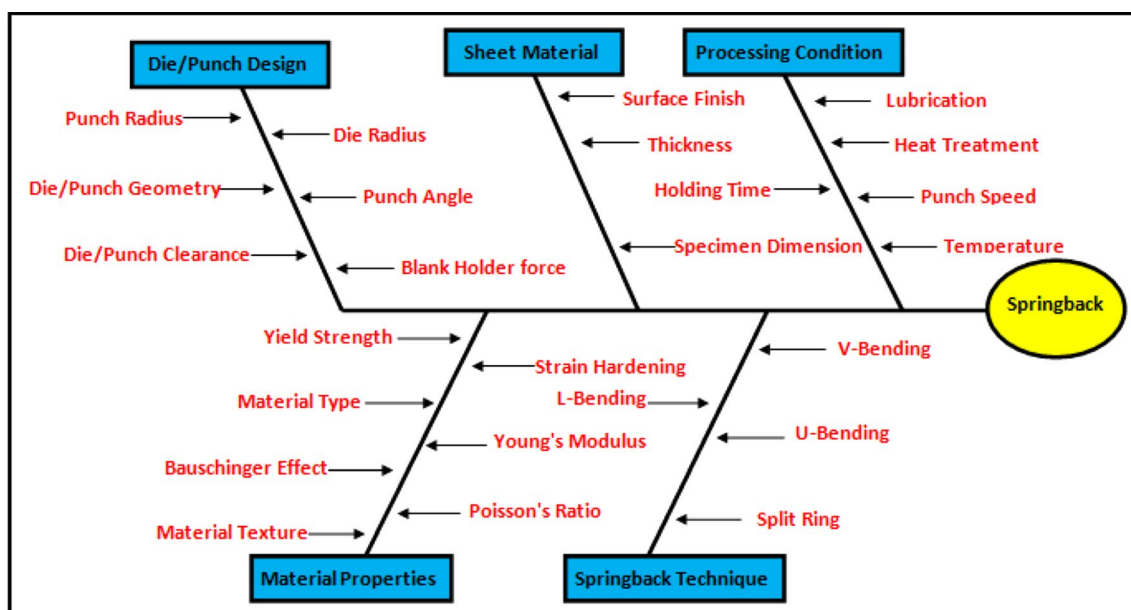


Fig. 1 Cause and effect diagram (Ishikawa diagram) for springback behavior



2 Experimental Details

2.1 Tensile Testing

A high-strength 1-mm-thick Inconel 625 alloy sheet was used for springback analysis, and its chemical composition is shown in Table 1. Mechanical properties were determined using tensile test specimen as per sub-size ASTM E08/E8M-11 standard. The tensile testing was carried out on a 100-kN Zwick Roell universal testing machine which has the advantage of a box furnace and non-contact type laser extensometer for recording the strain with high accuracy, as shown in Fig. 2.

The tensile testing was carried out on different temperatures (303 K, 473 K and 673 K) with sheet orientations (RD, ND and TD) and deformation speeds (1 mm/min, 5 mm/min and 10 mm/min). The representative tensile test specimen with different directions is shown in Fig. 3. Three specimens were tested for each setting, and their average values were taken into consideration for determination of mechanical properties. The long tensile test specimen as shown in Fig. 4 was used for finding Young’s modulus (E). It has been reported that long tensile test specimens help in accurate determination of the E value at high temperature conditions [17].

Table 1 Chemical composition of Inconel 625

Element	Ni	Cr	Nb	Mo	Ti	Al	Fe	Mn	Si
Weight (%)	61.495	21.739	3.271	9.479	0.166	0.067	3.304	0.123	0.101

Fig. 2 Zwick Roell 100kN UTM machine

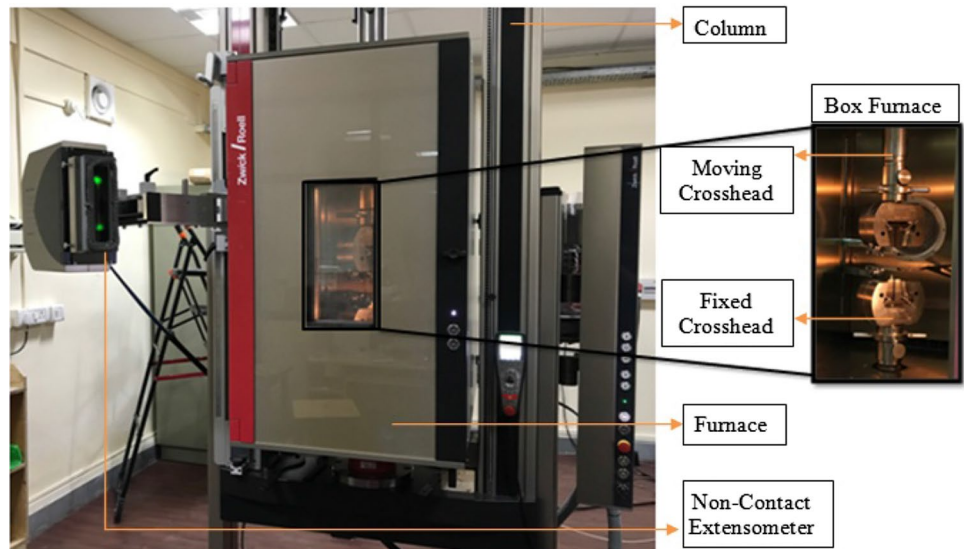
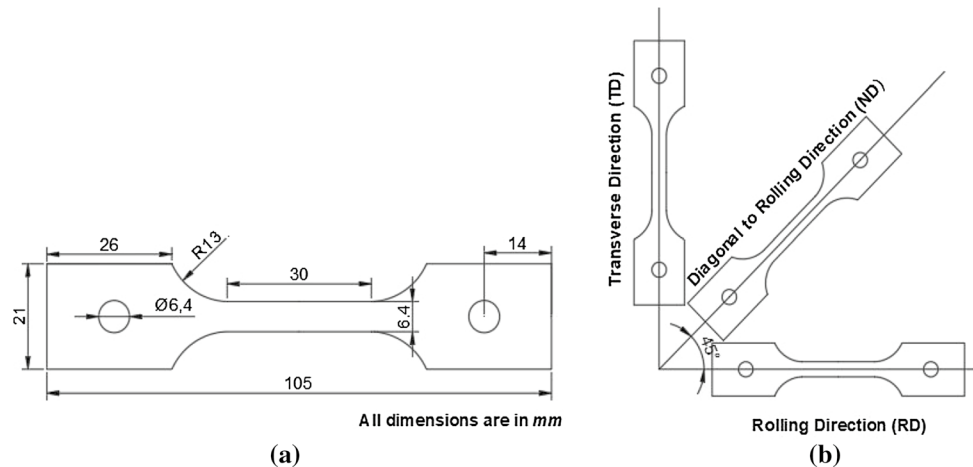


Fig. 3 Tensile test specimens **a** for testing and **b** with considered orientations



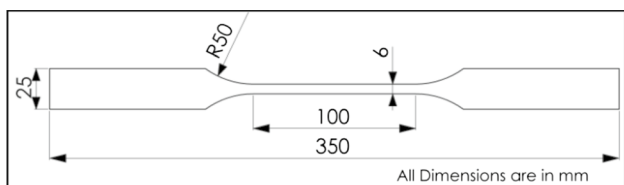


Fig. 4 Long tensile test specimens for determination of Young’s modulus

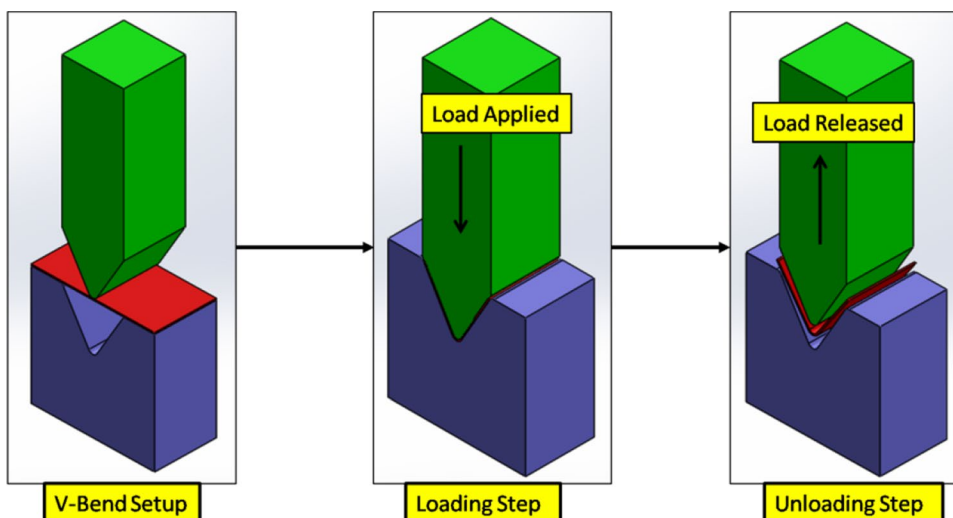


Fig. 5 Compression machine used for V-bending

Table 2 Process parameters with different levels of setting

Parameter	Level		
	Level 1	Level 2	Level 3
Temperature	303 K	473 K	673 K
Punch speed	1 mm/min	5 mm/min	10 mm/min
Holding time	30 s	60 s	90 s
Rolling direction	RD (0°)	TD (45°)	ND (90°)

Fig. 6 Schematic diagram of V-bending process



2.2 V-Bending

The V-bending for springback analysis was performed on a 100-kN compression testing machine as shown in Fig. 5. The die is fixed with a punch radius of 3 mm and a nose angle of 60°. All the tests were carried out in isothermal conditions. The rectangular strips of 80×40 mm were considered for V-bending. The design of experiments was based upon Taguchi (L_{27}) orthogonal array. Four process parameters with three different levels were taken into consideration as shown in Table 2. Three specimens were tested for each set of process parameters, and the average springback value was reported for analysis. The process of V-bending is shown in Fig. 6. The punch load is applied in the loading step, followed by the prescribed holding time and then the unloading step, in which the punch load is released, and the sheet attempts to regain its original shape.

3 Results and Discussion

3.1 Flow Stress and Material Properties Analysis

The true stress–strain plot for varying temperatures at a fixed deformation punch speed of 1 mm/min and sheet orientation in RD is shown in Fig. 7a. The flow stress of the material was observed to vary inversely with temperature. Deformation speed dependency of flow stress at fixed temperature of 673 K and sheet orientation in RD is shown in Fig. 7b. Deformation rate also shows inversely proportional behavior with flow stress. Rolling direction was also observed to have a major influence over the flow stress of the material. Figure 7c shows a representative plot for the variation of true stress–strain at a temperature of 673 K and 10 mm/min punch speed.

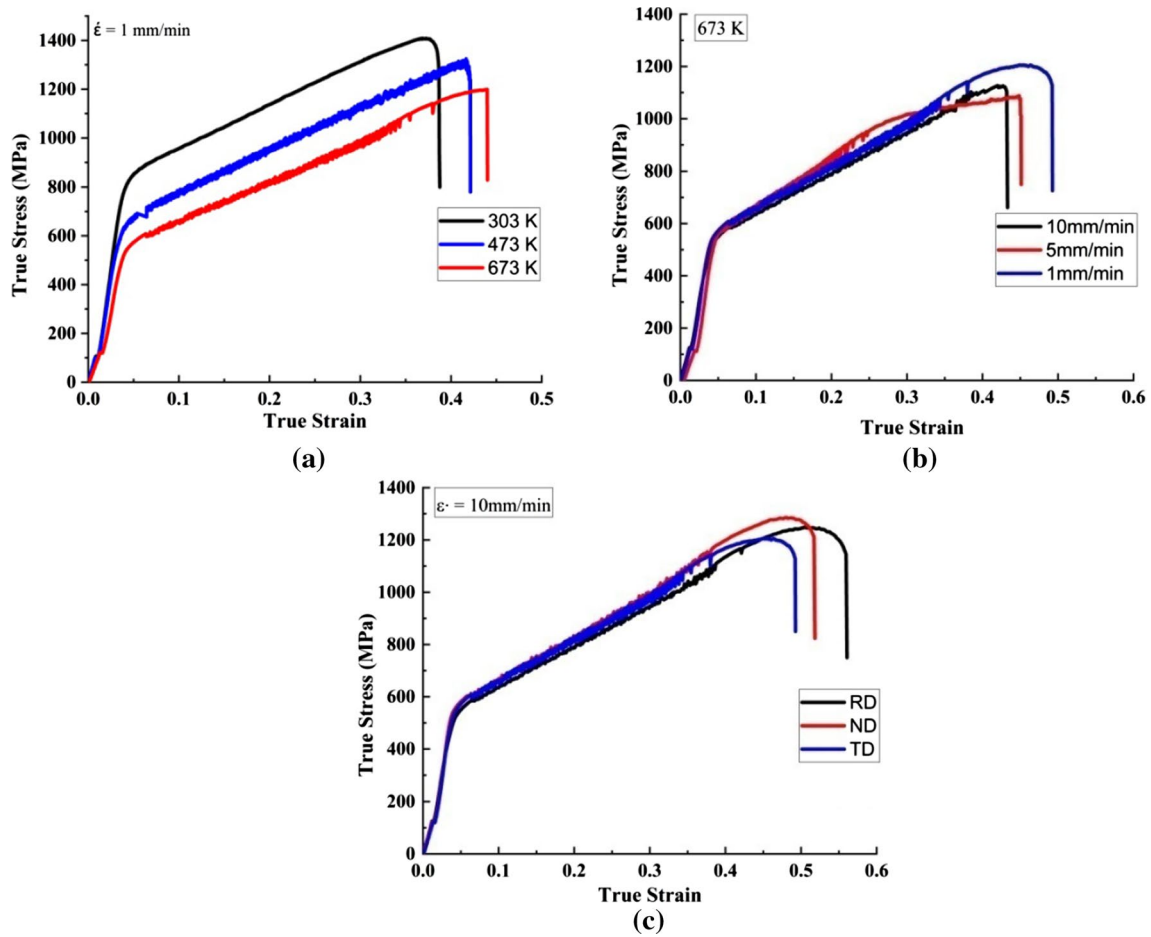


Fig. 7 Inconel 625 flow stress behavior with variation in **a** temperature, **b** deformation speed and **c** rolling direction of sheet

Average mechanical properties as calculated at different temperatures and 5 mm/min deformation speed are shown in Table 3. The ultimate and yield strength displayed a decrease of 18% and 25%, while the ductility of specimen increased by approximately 17% with temperature changing from 303 to 673 K. The exponent of strain hardening (n) and strength coefficient (K) were calculated with the help of Hollomon’s power law as shown in Eq. 1. Plastic anisotropy of any metal can be defined with the help of Lankford coefficient (R) as shown in Eq. 2. R can be represented as the ratio of strain for width upon thickness strain.

$$\sigma = K\epsilon^n \tag{1}$$

$$R = \frac{\epsilon_w}{\epsilon_t} \tag{2}$$

The Young’s modulus of Inconel 625 was obtained with the help of thin long tensile test specimen. Thin longer specimen is specifically used for this calculation as it is mentioned in previous literature by Saito et al. [17] who concluded that it allowed better accuracy for determining the Young’s modulus at high temperatures. The calculated

Table 3 Average mechanical properties of as-received Inconel 625

Temperature (K)	σ_{ys} (MPa)	σ_{ults} (MPa)	Percent elongation (%)	n	K (MPa)	Lankford coefficient		
						(R_0)	(R_{45})	(R_{90})
303	812.07 ± 5	978.55 ± 6	39.65 ± 0.3	0.31	1911.6	0.8515	0.9686	0.7490
473	691.73 ± 6	852.79 ± 8	42.99 ± 0.4	0.32	1718.1	0.8256	0.8518	1.3906
673	609.50 ± 6	805.18 ± 7	46.57 ± 0.5	0.34	1673.3	1.0869	0.6612	0.7043

Young's moduli at various considered temperatures are displayed in Table 4.

The microstructures of Inconel 625 in different orientations (RD, ND and TD) were taken using optical microscopes and are shown in Fig. 8. The average ASTM number observed for grain size was 9. Mechanical properties observed in RD at various temperatures were better than at the other two directions (TD and ND) because of grains which were fine and elongated. Carbide stringers were also observed in considerable abundance in the matrix of austenite, which might have occurred due to the procedure which was followed for solidification of metal and also due to various parameters such as the cooling rate, ratio of Nb/C in the alloy and time considered for solidification. Mitchell et al. [18] also reported carbide presence in eutectic form after final metal solidification.

3.2 V-Bending Analysis

3.2.1 Taguchi Analysis

The springback phenomenon plays a crucial role in sheet metal forming processes. Process parameters, namely temperature, punch speed, holding time and rolling direction, were considered for analysis of springback by L_{27} orthogonal array. The average angle of V-bend in each specimen is measured using Fig. 9 and is stated in Eq. 3. In Eq. 3, θ_1 and θ_2 are the angles for the inner and outer face of the V-bended sheet. Three different specimens were considered for each setting of parameters, and their average angle is reported in Table 4.

Table 4 Calculated Young's modulus

Temperature (K)	Young's modulus (GPa)
303	209.6 ± 7
473	202.8 ± 4
673	187.6 ± 5

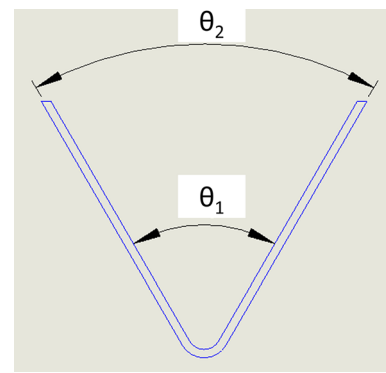


Fig. 9 Springback angle calculation

$$\theta' = \frac{(\theta_1 + \theta_2)}{2} \quad (3)$$

Analysis by the Taguchi method is often done by two measures, namely target performance measure (TPM) and noise performance measure (NPM) [12]. NPM helps in identifying the set of process parameters which reduces the variation in desired output values, and it does not affect the mean value at all. The S/N ratio is considered for analysis of NPM. Mean responses are often considered in TPM analysis. Mean responses are the average values of all the measures taken (three in the present case) for a set of parameters. The parameters which govern the NPM are known as variability process parameters, while the parameters which govern the TPM are known as target process parameters. The average springback angles are reported in Table 5.

Analysis of variance (ANOVA) is a statistical tool used to compare performance of each selected process parameter. It also gives a quantitative comparison, i.e., percentage contribution of each process parameter which helps in selecting the most influential parameter on the springback effect. The ANOVA table according to TPM analysis is represented in Table 6. In analysis of TPM, temperature (warm forming condition) had the greatest contribution toward minimizing

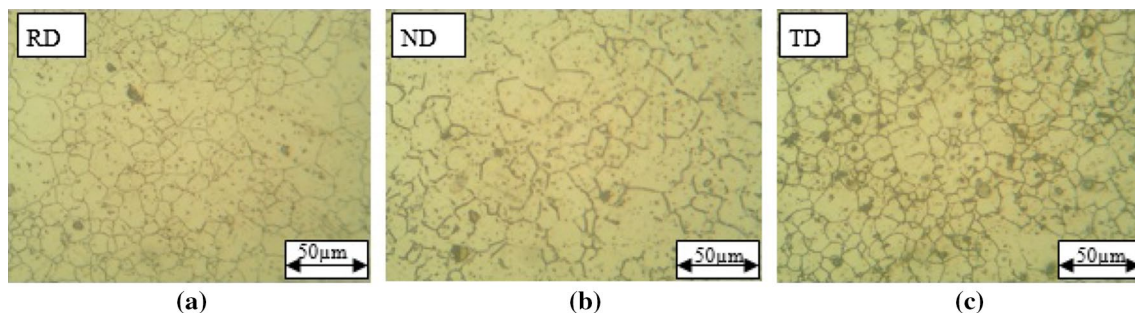


Fig. 8 Optical micrographs observed for Inconel 625 in **a** RD, **b** ND and **c** TD



Table 5 Springback angle and S/N ratio for different combinations of process parameters

Experiment number	Temperature	Punch speed	Holding time	Rolling direction	Avg. angle (θ_p)	S/N ratio
1	1	1	1	1	67.15	- 17.083
2	1	1	2	2	66.92	- 16.803
3	1	1	3	3	65.20	- 14.334
4	1	2	1	2	67.43	- 17.426
5	1	2	2	3	65.81	- 15.290
6	1	2	3	1	65.52	- 14.840
7	1	3	1	3	66.78	- 16.630
8	1	3	2	1	66.43	- 16.171
9	1	3	3	2	66.13	- 15.757
10	2	1	1	1	64.28	- 12.623
11	2	1	2	2	64.51	- 13.079
12	2	1	3	3	63.15	- 10.009
13	2	2	1	2	65.02	- 14.022
14	2	2	2	3	63.51	- 10.916
15	2	2	3	1	63.50	- 10.893
16	2	3	1	3	64.02	- 12.086
17	2	3	2	1	63.74	- 11.482
18	2	3	3	2	64.02	- 12.096
19	3	1	1	1	62.51	- 07.993
20	3	1	2	2	62.50	- 07.982
21	3	1	3	3	61.51	- 03.641
22	3	2	1	2	62.73	- 04.735
23	3	2	2	3	61.75	- 04.861
24	3	2	3	1	61.71	- 04.690
25	3	3	1	3	62.08	- 06.418
26	3	3	2	1	62.00	- 06.033
27	3	3	3	2	61.77	- 04.960

Table 6 ANOVA for TPM (mean springback response)

Source	Seq. SS	<i>p</i> value	% Contribution
Temperature	84.086	0.003	73.08
Punch speed	03.040	0.648	02.64
Holding time	15.003	0.006	13.03
Rolling direction	12.927	0.007	11.23
Total	115.056	-	100

the springback followed by holding time, rolling direction or sheet orientation and punch speed for Inconel 625 alloy.

Inconel 625 becomes soft with temperature increase and hence retains the deformed shape very easily. As observed in Fig. 10, springback reduces with an increase in temperature. Similar findings were also reported by Aerens and Dufloy [19]. The holding time after the loading step in V-bending also plays a very important role in reducing the springback effect as can be seen in Fig. 10, supporting previous observations made by Tekaslan et al. [20]. Texture and orientation of material also have an observable contribution to the

springback effect, which can be observed from Fig. 10, as well as the variation of springback angle with the orientations of the sheet. The highest springback is observed in the case where the grain orientation with the punch is at 45° (ND) followed by 0° (RD) and 90° (TD). However, in the present investigation, punch speed as a process parameter was found to have a negligible effect over springback [21, 22]. The level of process parameter having lower average springback angle is always preferred.

Table 7 shows the ranking of process parameters according to their contribution to reduce the springback effect. It could be clearly observed from the rank obtained for the process parameters in the response table that the temperature was the most influencing parameter in reduction in springback followed by holding time, sheet orientation and punch speed. Equally important statistically is to find the relation between each parameter and the response obtained, called the *p* value, which is shown in Table 6. The significance level chosen for *p* value analysis is 0.05 (5%). Parameters having *p* value lower than the significance level chosen for the present study, i.e., 0.05, are more statistically influencing the study

Fig. 10 Main effect plot for mean springback angle

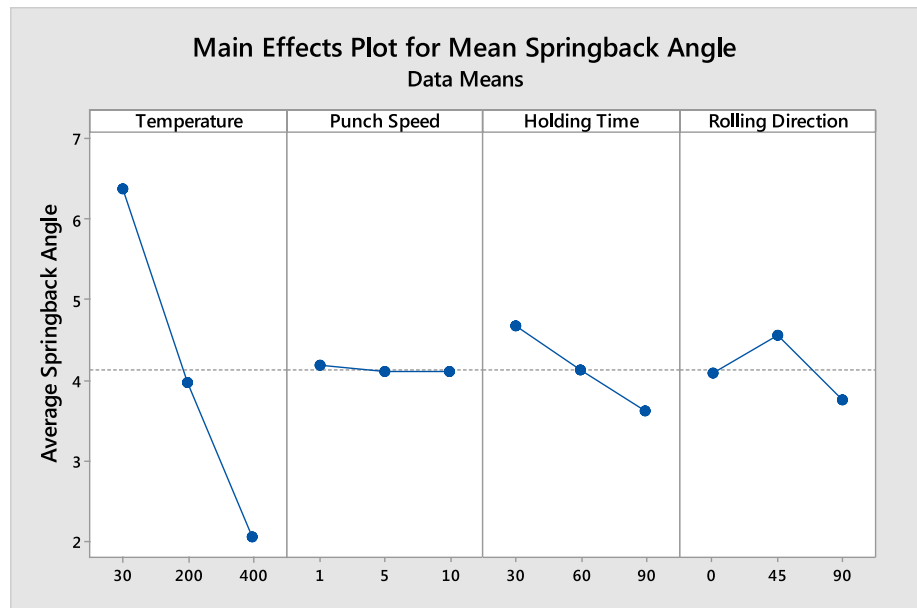


Table 7 Response table for TPM

	Temperature	Punch speed	Holding time	Rolling direction
Level 1	6.375	4.191	4.667	4.093
Level 2	3.972	4.109	4.130	4.560
Level 3	2.062	4.109	3.612	3.757
Delta	4.313	0.082	1.054	0.803
Rank	1	4	2	3

Table 9 Response table for NPM

	Temperature	Punch speed	Holding time	Rolling direction
Level 1	- 16.037	- 11.505	- 12.557	- 11.312
Level 2	- 11.912	- 11.297	- 11.402	- 12.318
Level 3	- 6.146	- 11.293	- 10.136	- 10.465
Delta	9.892	0.213	2.422	1.853
Rank	1	4	2	3

Table 8 ANOVA for NPM

Source	Seq. SS	p value	% Contribution
Temperature	191.218	0.011	46.99
Punch speed	10.970	0.976	02.62
Holding time	107.133	0.010	26.29
Rolling direction	98.061	0.075	24.09
Total	407.382	-	100

[23]. In the present work, temperature (0.3%), holding time (0.6%) and rolling direction (0.7%) have greater relevance than punch speed (64.8%) in reducing the springback effect.

In the case of NPM, from ANOVA, as shown in Table 8, it could be observed that temperature, holding time and rolling direction have a greater influence in maximizing the S/N ratio than the punch speed. Based upon the delta value in the response table for NPM, as shown in Table 9, a rank was attributed to the parameters that contribute to an increase in the S/N ratio. Hence, the temperature has the greater influence followed by holding time, rolling direction and punch speed in the case of NPM. NPM

analysis was carried out to identify the process parameter set which helps in reducing the variation in output response. S/N ratios are calculated on the basis of 'smaller is better' in MINITAB software as the objective is to reduce the springback [12]. The S/N ratios are calculated based upon Eqs. 4 and 5. On the basis of the S/N ratio calculation for each individual experiment, experiment 21 (temperature = 673 K, punch speed = 1 mm/min, holding time = 90 s and sheet rolling direction = 90°), as shown in Table 4, has the greater S/N ratio and could therefore be considered as the most optimal setting for reducing springback in the present work. However, an additional validation test was carried out.

$$S/N = -10 \times \log_{10}(\bar{y}^2) \tag{4}$$

$$\bar{y} = \sum_{i=1}^n y_i/n \tag{5}$$

Different process parameters were selected for the validation test on the basis of their relative contribution to

Table 10 Optimum level of each process parameter

Process parameter	TPM		NPM		Effect of factor (TPM or NPM)
	% contribution	Pooled	% contribution	Pooled	
Temperature	73.08	No	46.99	No	Both
Punch speed	02.64	Yes	02.62	Yes	Neither
Holding time	13.03	No	26.29	No	Both
Rolling direction	11.23	No	24.09	No	Both

Table 11 Optimum settings for each process parameter

Process parameter	TPM		NPM		Selected level	Actual value
	level	% Contribution	level	% contribution		
Temperature	3	73.08	3	46.99	3	673 K
Punch speed	1	02.64	3	02.62	1	1 mm/min
Holding time	3	13.03	3	26.29	3	90 s
Rolling direction	3	11.23	3	24.09	3	90°

minimize the springback effect. The condition for pooled and not pooled is considered based on the percentage contribution of that particular process parameter in TPM and NPM analysis. For the present study, pooling condition is preferred to be 5%. The influence that each distinct factor has on the relative contribution for NPM and TPM analyses is shown in Table 10. In case of punch speed, TPM (2.64%) and NPM (2.62%) contribution is less than 5%; hence, it is considered to be pooled. Conversely, if a process parameter is not pooled in either NPM or TPM analysis, then it is considered to have the most significant contribution in reduction in springback, such as temperature, punch velocity and holding time of blank. Among NPM and TPM, whichever is having the highest percentage contribution toward reduction in springback is considered for further analysis in confirmation test. In the present case, TPM is considered for temperature, and NPM is considered for holding time and rolling direction of sheet as shown in Table 11.

The set of process parameters for the test was as follows: temperature = 673 K, punch speed = 1 mm/min, holding time = 90 s and rolling direction = 90°. The conformation test was repeated three times, and springback results are presented in Table 12.

The *t*-distribution (*t* test) and *z*-distribution (*z* test) tests were conducted with confidence interval of 95% for calculation of mean springback angle on the basis of the available fixed sample size. For larger sample sizes, the *z*-test is preferable. However, for the small sample size, *t*-tests were carried to get accurate results [24]. The tolerance and range were calculated and presented for both experimental and validation cases as shown in Table 13. The mean springback was reduced by 69.63% as we moved from the experimental to the validation test. The range for confidence level of 95% also showed improvement by approximately 67%.

Table 12 V-bending results for validation test

Experiment	Die angle, θ_i	Spring-back angle θ_f	$\Delta\theta = \theta_f - \theta_i$	Average $\Delta\theta$
Iteration 1	60°	61.26°	1.26°	1.25°
Iteration 2		61.35°	1.35°	
Iteration 3		61.16°	1.16°	

3.2.2 Bending Moment Analysis in Springback

As observed by the Taguchi analysis, springback is primarily affected by temperature. In general, the springback amount is reported using a springback ratio as shown in Eq. 6. The angle of the die is $\theta_i = 60^\circ$. Bending moment also plays a major role in springback analysis. The springback factor is directly proportional to the bending moment applied and the flow stress ($\bar{\sigma}$) of the material as stated by Saito et al. [17] and shown in Eq. 7.

$$\text{Springback ratio} = \frac{\theta_f - \theta_i}{\theta_i} = \frac{\Delta\theta}{\theta_i} \tag{6}$$

$$\frac{\Delta\theta}{\theta_i} = \frac{M}{EI} \propto \frac{\bar{\sigma}}{E} \tag{7}$$

Springback of any material can be said to be inversely proportional to the Young’s modulus (*E*) and directly proportional to the flow stress of material. The load (*P*) for bending the sheet is also directly proportional to the springback factor, as expressed in Eq. 8.

Table 13 Confidence test results

Results	Test criteria	Total test	Mean	Standard deviation	95% Confidence interval	Range	Tolerance
Experimental	z test	81	4.136	0.364	$3.423 < \theta_{\text{exp}} < 4.849$	1.426	4.136 ± 0.713
Validation	t test	3	1.256	0.095	$1.020 < \theta_{\text{confi}} < 1.492$	0.472	1.256 ± 0.236

$$\frac{\Delta\theta}{\theta_i} \propto \frac{\bar{\sigma}}{E} \propto \frac{P}{E} \quad (8)$$

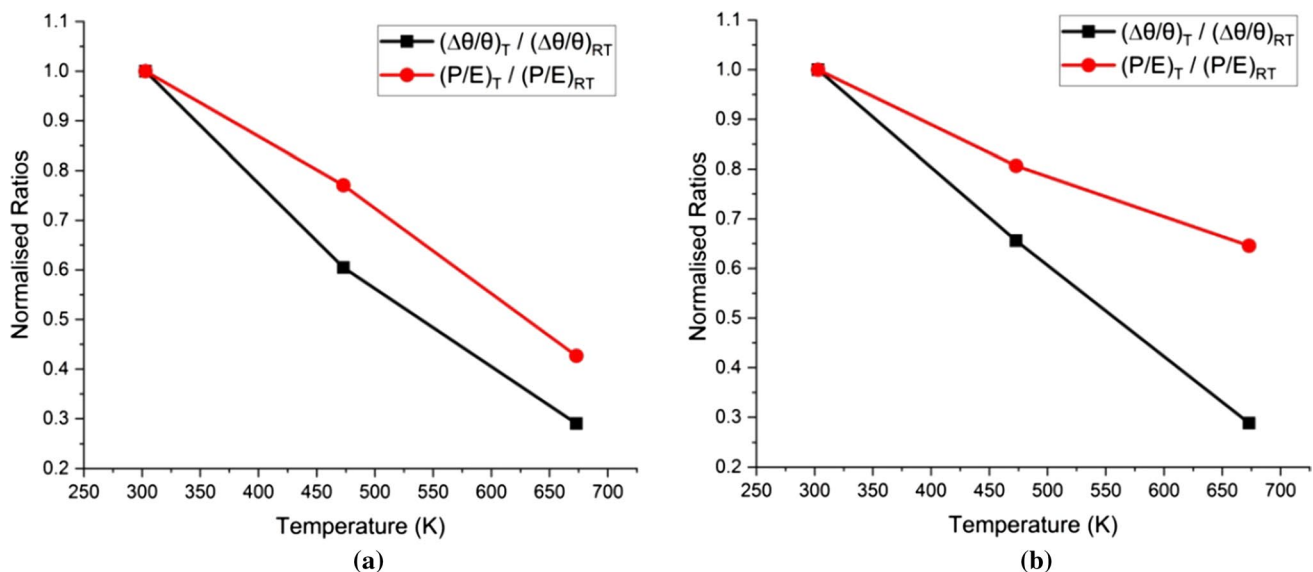
Normalized ratio (P/E) and springback angle ratio ($\Delta\theta_T/\Delta\theta_{RT}$) play a crucial role in springback behavior of material. These factors are highly dependent on forming temperature and punch speed. The other factors such as Young's modulus, bending stress and viscoplastic behavior also contribute effectively toward the springback analysis of material [16]. These ratios are evaluated and line graphs are drawn for comparing the slopes of lines at two different punch velocities (1 mm/min and 10 mm/min) as shown in Fig. 11 a, b. At low punch velocity (1 mm/min) during the unloading step, it was observed that the reduction in the P/E ratio is smaller when compared to the ratio of angle ($\Delta\theta_T/\Delta\theta_{RT}$), which may be due to the role of viscoplastic factors such as creep and stress relaxation at the time of unloading. However, at high punch velocity (10 mm/min), quick unloading takes place, and the springback of the material only depends upon properties such as Young's modulus, bending stress and temperature. The similar observations were also reported by Saito et al., for precipitation strengthened steel [17].

3.2.3 Springback Factor (K_s)

The main reason for springback is deformation of metal in the elasto-plastic region of the material and is primarily influenced by work hardening, rolling conditions and the elastic behavior of material. Springback factor (K_s), as shown in Eq. 9, helps in calculating the total springback of metal at considered working conditions.

$$K_s = \frac{\theta_i}{\theta_f} = \frac{R_f + 0.5t}{R_i + 0.5t} \quad (9)$$

In this equation, θ_f is angle after bending, θ_i is the initial die angle, R_f is the radius of fillet after bending, R_i is the punch nose radius and t is the sheet thickness. Pure elastic recovery is expected in case K_s is 0, and no springback is reported in case K_s is 1. As the R_f/t ratio is fixed, K_s is compared with the different process parameters considered in the present study. Separate tests were performed for individual comparison of each parameter with all other fixed process parameters. Representative graphs of these comparisons are shown in Fig. 12a–d. Figure 13a–d shows V-bend specimens for individual comparisons of springback for different

**Fig. 11** Comparison of normalized ratios and temperature at **a** low speed (1 mm/min) and **b** high speed (10 mm/min)

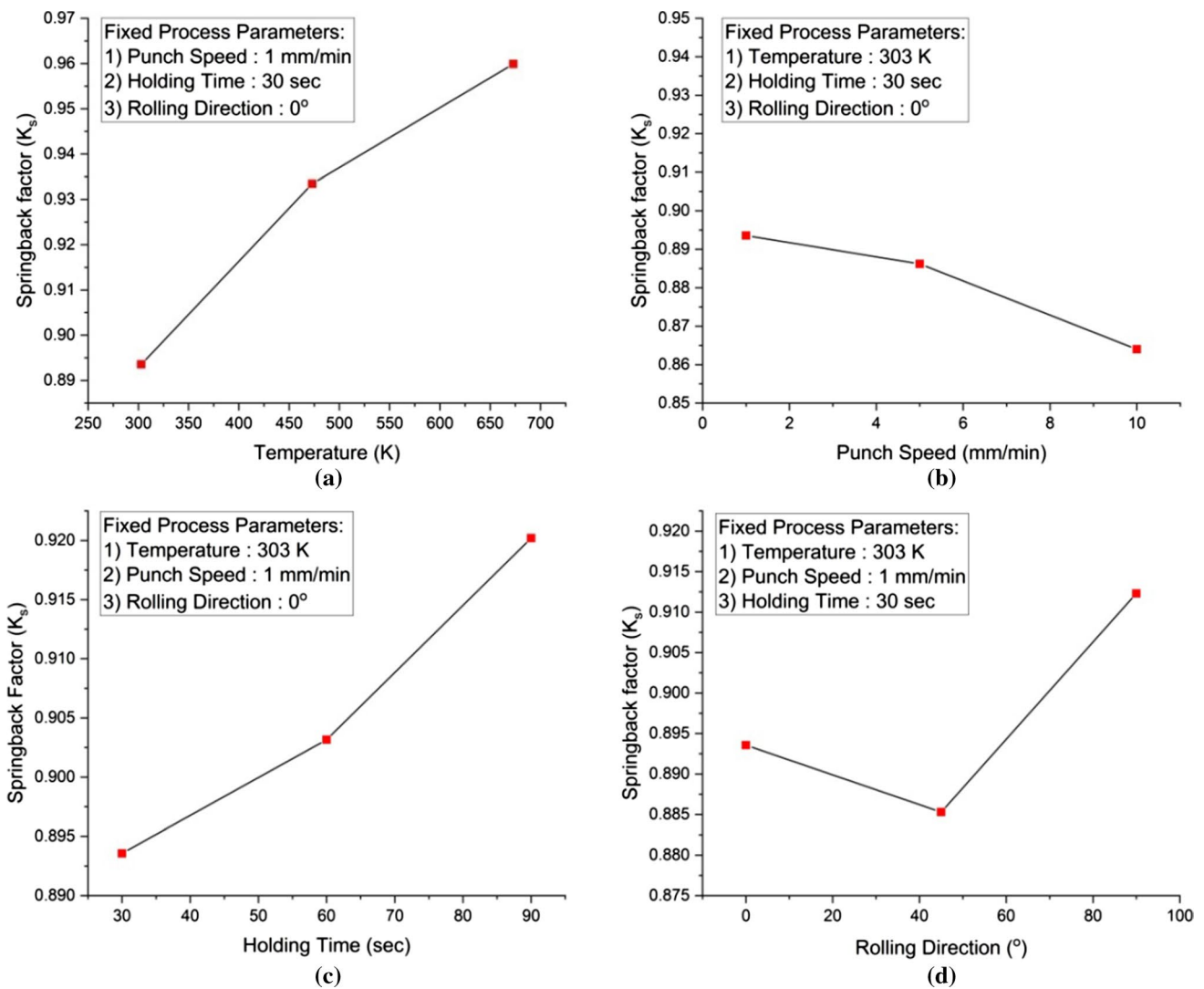


Fig. 12 Variation of springback factor with a temperature, b punch speed, c holding time and d rolling direction of sheet

process parameters, and similar trends were followed for other levels of process parameters considered in the present study.

The springback factor showed improvement with the increase in temperature and holding time, but decreased with increments in punch speed. Nothing particular was observed with respect to orientation angle of the sheet. With the increase in temperature, the ductility increased which, in turn, helped in reducing the elastic core and the bending stress, which are both needed for springback. Punch holding time gives ample amount of time to the deformed material to gain new shape, and hence, springback reduces with increases in holding time. Orientation and texture of material also played an important role in the material springback. No particular trend was noted with regard to sheet orientation. Greater springback was found for TD (45°) orientation sheet followed by RD (0°) and ND (90°). In the case of punch

velocity, the lower it is, the smaller will be the springback as the material will have sufficient time to rearrange its grains while bending takes place.

3.3 Finite Element Analysis

Numerical simulations were done for all 27 experiments using the same set of process parameters as mentioned in Table 5. User-defined material (UMAT) subroutine was incorporated in numerical solver ABAQUS 6.13 for FEA. The die and punch were modeled using a discrete rigid type, in which a rigid body reference node controls the whole movement. R3D4 type of mesh elements was used. The deformable blank was meshed using S4 mesh element which is a 4-node shell element used for thin sheet analysis. In forming of sheet metals, planar anisotropy and constitutive models play a major role, and hence, anisotropic

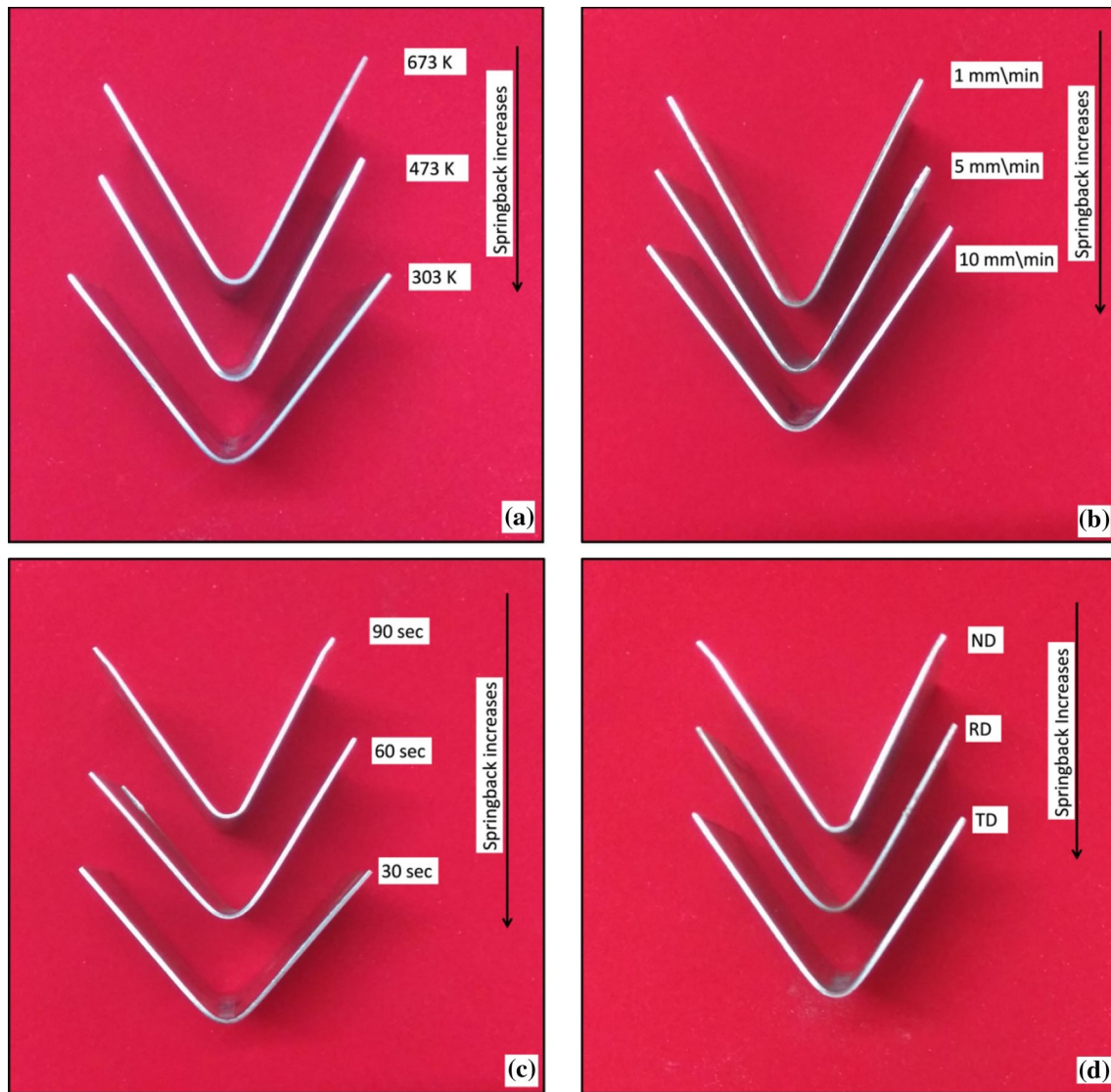


Fig. 13 Variation of springback with **a** temperature, **b** punch speed, **c** holding time and **d** sheet orientation

Table 14 Mesh sensitivity analysis

Mesh description	Simulation results	
	Springback angle	CPU run-time (s)
Uniform mesh with size $5 \times 5 \text{ mm}^2$	69.16°	1996
Uniform mesh with size $2.5 \times 2.5 \text{ mm}^2$	68.52°	3659
Uniform mesh with size $1 \times 1 \text{ mm}^2$	68.28°	7826
Mesh with size 1 mm over blank and 0.4 mm near fillet region	67.58°	9508

Experimental springback: 67.15°

Comparison Case Room temperature, punch speed=1 mm/min, holding time=30 s and sheet orientation=0° (RD)

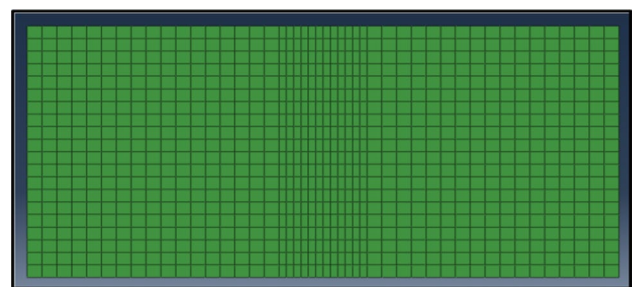


Fig. 14 Meshed blank considered for FEA

yield criteria were applied for Inconel 625 at various considered temperatures and rates of deformation. Two yield criteria, namely Hill 1948 [25] and Barlat 1989 [26], were applied and compared with the help of procedure followed in

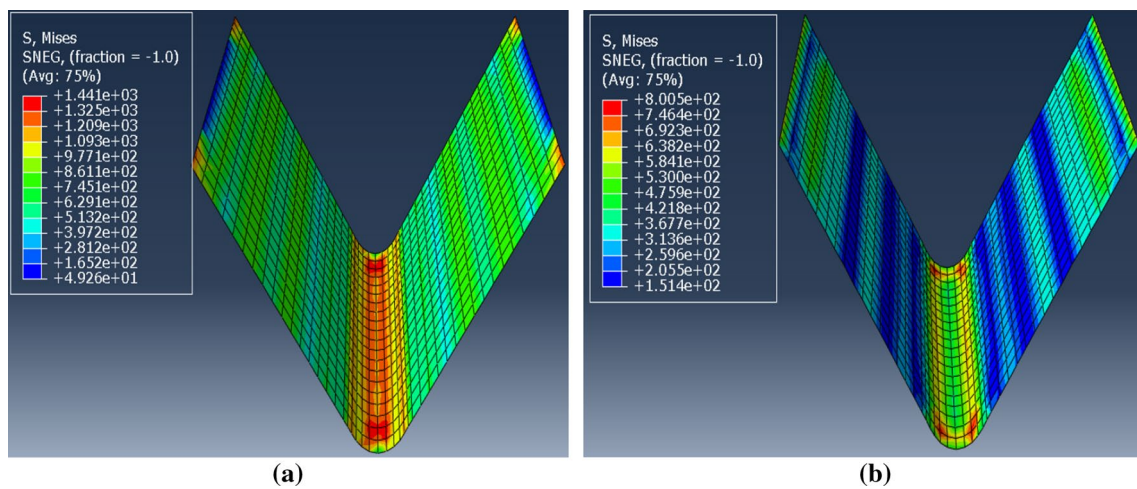


Fig. 15 FEA simulation with optimized parameter setting for a loading step and b unloading step

Table 15 Springback percentage of experimental and FEA results

Exp. no	Experimental springback (%)	FEA + Barlat 1989 springback (%)	FEA + Hill 1948 springback (%)	% Relative error for springback (Exp. vs. Barlat 1989)	% Relative error for springback (Exp. vs. Hill 1948)
1	11.91	12.37	12.60	3.82	5.78
2	11.53	11.77	12.08	2.07	4.82
3	8.67	8.92	8.60	2.82	0.83
4	12.39	12.15	12.80	1.93	3.32
5	9.68	9.52	9.37	1.72	3.27
6	9.19	9.32	8.98	1.33	2.30
7	11.31	11.43	11.63	1.13	2.90
8	10.72	10.58	10.52	1.30	1.92
9	10.22	10.38	10.50	1.58	2.72
10	7.13	7.42	7.48	4.05	4.99
11	7.51	7.72	7.30	2.74	2.81
12	5.24	5.47	5.65	4.24	7.73
13	8.37	8.60	8.77	2.79	4.78
14	5.85	6.03	5.65	3.13	3.42
15	5.83	6.03	6.12	3.43	4.86
16	6.70	6.77	6.92	1.00	3.23
17	6.24	6.33	6.08	1.51	2.49
18	6.71	6.90	6.98	2.90	4.14
19	4.18	4.37	4.53	4.52	8.51
20	4.17	4.20	4.38	0.67	5.06
21	2.52	2.47	2.70	1.99	7.28
22	4.56	4.65	4.37	2.07	4.15
23	2.91	3.05	3.05	4.77	4.77
24	2.85	2.82	2.90	1.17	1.75
25	3.47	3.48	3.60	0.48	3.85
26	3.33	3.37	3.55	1.00	6.50
27	2.94	2.88	3.10	2.08	5.28
Average relative error				2.30	4.21

previous work by Kotkunde et al. [27]. Also, Arrhenius constitutive model material constants were taken from authors' previous work done for deep drawing of Inconel 625 [27]. The UMAT code was formulated based on Arrhenius constitutive model with Hill 1948 and Barlat 1989 yield criteria for finite element analysis.

A mesh convergence study [28, 29] was done to fix the type and size of elements for achieving high level of accuracy for springback. The trials of mesh sensitivity with different mesh over blanks are shown in Table 14. The optimum mesh size was chosen on the basis of von Mises stress and springback angle obtained and compared with the experimental results. Another important factor considered during sensitivity analysis of mesh was the total computation time. The selected mesh has 0.4 mm size near fillet and 1 mm on the rest of the blank. A mesh with a total of 928 elements, as shown in Fig. 14, was generated for modeling the blank.

Numerical analysis of springback for V-bending was carried out to verify the experimental springback results. FEA was performed in three steps, namely loading step, holding step and unloading step. The representative numerical simulation of V-bending for the optimized setting (temperature = 673 K, punch speed = 1 mm/min, holding time = 90 s and rolling direction = 90°) with Barlat 1989 yield criteria is shown in Fig. 15. The observed angle after the unloading step in Fig. 15b was 61.28°. The unloading step is a stress-relieving one, and hence, it could be clearly observed that the von Mises stress reduced in the unloading step when compared to the loading one. Comparison for percentage springback calculated on the basis of Eq. 10 for experimental and FE simulations with incorporated yield criteria is presented in Table 15.

$$\% \text{springback} = \frac{\text{springback}}{\text{die angle}} \times 100 \quad (10)$$

It was found that the use of different yield criteria does not affect the results obtained for springback behavior of the metal sheet. The relative error for all the experiments of the Arrhenius constitutive model with Barlat 1989 yield criteria in FEA when compared to the experimental springback results was well within 5% of the acceptable range. On the basis of average relative percentage error, better prediction capability of springback is shown by Barlat 1989 rather than Hill 1948 yield criteria. Temperature and holding time are the two parameters having maximum influence over springback of Inconel 625 alloy; hence, the springback percentage also decreased with an increase in temperature and holding time.

4 Conclusions

The present work includes process parameter optimization for V-bending with the help of Taguchi Analysis for Inconel 625 alloy. FEA incorporated with different yield criteria was used for validating the experimentally obtained results.

Some of the important conclusions drawn from present work are:

- Different material properties are significantly affected by the rate of deformation, sheet orientation and working temperature. Yield and ultimate strength of material displayed an inversely proportional relationship, while elongation percentage displayed directly proportional relationships with temperature and rate of deformation.
- Taguchi L_{27} orthogonal array was used for process parameter optimization in order to minimize the springback effect. Based on the ANOVA for means and S/N ratio for springback effect, it has been observed that temperature was the most influential parameter followed by holding time, orientation of sheet and punch speed. The optimum set of parameters (temperature of 673 K, punch speed of 1 mm/min, holding time of 90 s and sheet orientation of 90°) was obtained from Taguchi analysis and used for the validation test. With these set of parameters, the amount of springback angle reduced by approximately 69.63%.
- Springback effect was found to be inversely proportional to holding time and temperature but directly proportional to the punch speed. Nothing particular could be said about the relationship between sheet orientation and springback angle from the present study as the greater springback was observed TD (45°) followed by RD (0°) and ND (90°).
- Bending moment of the sheet also plays an important role in the V-bending process. It was found that at low speed, some additional factors such as creep and stress relaxation at the time of unloading play a major role. However, at high speed, quick unloading takes place, and the springback depends only on Young's modulus, bending stress and temperature.
- The UMAT code was written based on the Arrhenius constitutive model with Hill 1948 and Barlat 1989 yield criteria for finite element analysis. Springback percentage was evaluated, and Barlat 1989 displayed better prediction capability. Relative percentage error of springback for Barlat 1989 criteria with respect to the experimental results was well within the 5% of acceptance range.

Acknowledgements The authors are grateful to the BITS, Hyderabad for permitting the use of UTM facility at the Central Analytical Lab

(CAL) and also acknowledge SERB–DST ECR, Government of India (ECR/2016/001402), for funding this research project.

Compliance with Ethical Standards

Conflict of interest The authors declare that they have no conflict of interest.

References

- Lin, Y.C.; Yang, H.; Xin, Y.; Li, C.-Z.: Effects of initial microstructures on serrated flow features and fracture mechanisms of a nickel-based superalloy. *Mater. Charact.* **144**, 9–21 (2018). <https://doi.org/10.1016/j.matchar.2018.06.029>
- Prasad, K.S.; Panda, S.K.; Kar, S.K.; Murty, S.V.S.N.; Sharma, S.C.: Effect of solution treatment on deep drawability of IN718 sheets: experimental analysis and metallurgical characterization. *Mater. Sci. Eng. A.* **727**, 97–112 (2018). <https://doi.org/10.1016/j.msea.2018.04.110>
- Shoemaker, L.E.: Alloys 625 and 725: trends in properties and applications. In: *Superalloys 718, 625, 706 and Various Derivatives*. pp. 409–418. TMS (2005)
- Pandre, S.; Kotkunde, N.; Takalkar, P.; Morchhale, A.; Sujith, R.; Singh, S.K.: Flow stress behavior, constitutive modeling, and microstructural characteristics of DP 590 steel at elevated temperatures. *J. Mater. Eng Perform.* **28**, 7565–7581 (2019). <https://doi.org/10.1007/s11665-019-04497-y>
- Jeswiet, J.; Geiger, M.; Engel, U.; Kleiner, M.; Schikorra, M.; Dufloy, J.; Neugebauer, R.; Bariani, P.; Bruschi, S.: Metal forming progress since 2000. *CIRP J. Manuf. Sci. Technol.* **1**, 2–17 (2008). <https://doi.org/10.1016/j.cirpj.2008.06.005>
- Zhang, D.; Cui, Z.; Ruan, X.; Li, Y.: An analytical model for predicting springback and side wall curl of sheet after U-bending. *Comput. Mater. Sci.* **38**, 707–715 (2007). <https://doi.org/10.1016/j.commatsci.2006.05.001>
- Ramadass, R.; Sambasivam, S.; Thangavelu, K.: Selection of optimal parameters in V-bending of Ti-Grade 2 sheet to minimize springback. *J. Braz. Soc. Mech. Sci. Eng.* **41**, 21 (2019). <https://doi.org/10.1007/s40430-018-1521-x>
- Bakhshi-Jooybari, M.; Rahmani, B.; Daezadeh, V.; Gorji, A.: The study of spring-back of CK67 steel sheet in V-die and U-die bending processes. *Mater. Des.* **30**, 2410–2419 (2009). <https://doi.org/10.1016/j.matdes.2008.10.018>
- Zong, Y.; Liu, P.; Guo, B.; Shan, D.: Springback evaluation in hot v-bending of Ti–6Al–4V alloy sheets. *Int. J. Adv. Manuf. Technol.* **76**, 577–585 (2015). <https://doi.org/10.1007/s00170-014-6190-z>
- Thippakmas, S.; Phanitwong, W.: Process parameter design of spring-back and spring-go in V-bending process using Taguchi technique. *Mater. Des.* **32**, 4430–4436 (2011). <https://doi.org/10.1016/j.matdes.2011.03.069>
- Verma, R.K.; Haldar, A.: Effect of normal anisotropy on spring-back. *J. Mater. Process. Technol.* **190**, 300–304 (2007). <https://doi.org/10.1016/j.jmatprotec.2007.02.033>
- Choudhury, I.A.; Ghomi, V.: Springback reduction of aluminum sheet in V-bending dies. *Proc. Inst. Mech. Eng. Part B: J. Eng. Manuf.* (2014). <https://doi.org/10.1177/0954405413514225>
- Panthi, S.K.; Ramakrishnan, N.; Das Gupta, R.; Chouhan, J.S.: Study of effect of load on springback in sheet metal bending. *Trans. Indian Inst. Met.* **61**, 39–43 (2008). <https://doi.org/10.1007/s12666-008-0063-9>
- Thippakmas, S.; Rojananan, S.: Investigation of spring-go phenomenon using finite element method. *Mater. Des.* **29**, 1526–1532 (2008). <https://doi.org/10.1016/j.matdes.2008.02.002>
- Narasimhan, N.; Lovell, M.: Predicting springback in sheet metal forming: an explicit to implicit sequential solution procedure. *Finite Elem. Anal. Des.* **33**, 29–42 (1999). [https://doi.org/10.1016/S0168-874X\(99\)00009-8](https://doi.org/10.1016/S0168-874X(99)00009-8)
- Forcellese, A.; Fratini, L.; Gabrielli, F.; Micari, F.: Computer aided engineering of the sheet bending process. *J. Mater. Process. Technol.* **60**, 225–232 (1996). [https://doi.org/10.1016/0924-0136\(96\)02334-5](https://doi.org/10.1016/0924-0136(96)02334-5)
- Saito, N.; Fukahori, M.; Minote, T.; Funakawa, Y.; Hisano, D.; Hamasaki, H.; Yoshida, F.: Elasto-viscoplastic behavior of 980 MPa nano-precipitation strengthened steel sheet at elevated temperatures and springback in warm bending. *Int. J. Mech. Sci.* **146–147**, 571–582 (2018). <https://doi.org/10.1016/j.ijmecsci.2017.11.044>
- Mitchell, A.M.W.: The precipitation of primary carbides in IN718 and its relation to solidification conditions. In: *Superalloys 718, 625, 706 and Derivatives*, pp. 299–310 (2005).
- Dufloy, J.R.; Aereens, R.: Force reduction in bending of thick steel plates by localized preheating. *CIRP. Ann.* **55**, 237–240 (2006). [https://doi.org/10.1016/S0007-8506\(07\)60406-5](https://doi.org/10.1016/S0007-8506(07)60406-5)
- Tekaslan, Ö.; Gerger, N.; Şeker, U.: Determination of spring-back of stainless steel sheet metal in “V” bending dies. *Mater. Des.* **29**, 1043–1050 (2008). <https://doi.org/10.1016/j.matdes.2007.04.004>
- Meinders, T.; Burchitz, I.A.; Bonte, M.H.A.; Lingbeek, R.A.: Numerical product design: springback prediction, compensation and optimization. *Int. J. Mach. Tools. Manuf.* **48**, 499–514 (2008). <https://doi.org/10.1016/j.ijmactools.2007.08.006>
- Samuel, M.: Experimental and numerical prediction of spring-back and side wall curl in U-bendings of anisotropic sheet metals. *J. Mater. Process. Technol.* **105**, 382–393 (2000). [https://doi.org/10.1016/S0924-0136\(00\)00587-2](https://doi.org/10.1016/S0924-0136(00)00587-2)
- Reddy, A.C.S.; Rajesham, S.; Reddy, P.R.; Kumar, T.P.; Goverdhan, J.: An experimental study on effect of process parameters in deep drawing using Taguchi technique. *Int. J. Eng. Sci. Technol.* **7**, 21–32 (2015)
- Massey, A.; Miller, S.J.: *Tests of Hypotheses Using Statistics*, p. 32. Brown University, Providence (2006)
- Hill, R.: Constitutive modelling of orthotropic plasticity in sheet metals. *J. Mech. Phys. Solids* **38**, 405–417 (1990). [https://doi.org/10.1016/0022-5096\(90\)90006-P](https://doi.org/10.1016/0022-5096(90)90006-P)
- Barlat, F.; Brem, J.C.; Yoon, J.W.; Chung, K.; Dick, R.E.; Lege, D.J.; Pourboghrat, F.; Choi, S.-H.; Chu, E.: Plane stress yield function for aluminum alloy sheets—part 1: theory. *Int. J. Plast.* **19**, 1297–1319 (2003). [https://doi.org/10.1016/S0749-6419\(02\)00019-0](https://doi.org/10.1016/S0749-6419(02)00019-0)
- Kotkunde, N.; Badrish, A.; Morchhale, A.; Takalkar, P.; Singh, S.K.: Warm deep drawing behavior of Inconel 625 alloy using constitutive modelling and anisotropic yield criteria. *Int. J. Mater. Form.* (2019). <https://doi.org/10.1007/s12289-019-01505-3>
- Morchhale, A.: Design and finite element analysis of hydrostatic pressure testing machine used for ductile iron pipes. *MER.* **6**, 23 (2016). <https://doi.org/10.5539/mer.v6n2p23>
- Morchhale, A.: Study of positioning and dimensional optimization of angled stiffeners using finite element analysis of above ground storage tank. *Int. J. Res. Mech. Eng.* **5**, 10–19 (2017)

